Monte Carlo calculations of the elastic moduli and pressure-volume-temperature equation of state for hexahydro-1,3,5-trinitro-1,3,5-triazine

Thomas D. Sewell[a)]
Theoretical Division, Los Alamos National Laboratory, Los Alamos, New Mexico 87545

Carl M. Bennett
Department of Chemistry, Oklahoma State University, Stillwater, Oklahoma 74078

(Received 27 September 1999; accepted for publication 10 February 2000)

Isothermal-isobaric Monte Carlo calculations were used to obtain predictions of the elastic coefficients and derived engineering moduli and Poisson ratios for crystalline hexahydro-1,3,5-trinitro-1,3,5-triazine (RDX). The elastic coefficients were computed using the strain fluctuation formula due to Rahman and Parrinello [J. Chem. Phys. **76**, 2662 (1982)]. Calculations were performed as a function of temperature ($218\,\mathrm{K} \leqslant T \leqslant 333\,\mathrm{K}$) and hydrostatic pressure ($0\,\mathrm{GPa} \leqslant p \leqslant 4\,\mathrm{GPa}$). The predicted values of the moduli and Poisson ratios under ambient conditions are in accord with general expectations for molecular crystals and with a very recent, unpublished determination for RDX. The moduli exhibit a sensitive pressure dependence whereas the Poisson ratios are relatively independent of pressure. The temperature dependence of the moduli is comparable to the precision of the results. However, the crystal does exhibit thermal softening for most pressures. An additional product of the calculations is information about the pressure-volume-temperature (pVT) equation of state. We obtain near-quantitative agreement with experiment for the case of hydrostatic compression and reasonable, but not quantitative, correspondence for thermal expansion. The results indicate a significant dependence of the thermal expansion coefficients on hydrostatic pressure. © *2000 American Institute of Physics.* [S0021-8979(00)03010-3]

I. INTRODUCTION

Plastic-bonded explosives (PBXs) and propellants are highly filled composite materials comprised of grains of an energetic material held together by a polymeric binder. There has been an increasing effort in recent years to understand and predict the macroscopic response of these composites on the basis of fundamental chemical, thermophysical and mechanical properties of, and interactions among, the constituents. This is a severe challenge due to both the large domain of spatio-temporal scales that must be spanned and the distinct classes of materials that must be described within a single modeling framework.

Our main interest is in the use of atomistic methods to predict the kinds of physical and mechanical properties required in the formulation and parameterization of detailed mesomechanics models which describe materials at the level of interacting constituents (e.g., grains and binder in a PBX). These methods are increasingly used to obtain constitutive laws for continuum calculations. As mesomechanics models become more sophisticated, there is a need for a more complete description of constituent properties, e.g., specification of the Young's moduli rather than the bulk modulus; and dependencies of the thermophysical properties on temperature, pressure, and strain rate.

In a preceding publication, we presented isothermal-isobaric (NpT) Monte Carlo calculations of the room-temperature, hydrostatic compression of hexahydro-1,3,5-trinitro-1,3,5-triazine (RDX) and β-octahydro-1,3,5,7-tetranitro-1,3,5,7-tetrazocine (β-HMX) within an all-atom rigid-molecule framework.[1] Hydrostatic pressures of $0\,\mathrm{GPa} \leqslant p \leqslant 3.95\,\mathrm{GPa}$ and $0\,\mathrm{GPa} \leqslant p \leqslant 7.47\,\mathrm{GPa}$ were considered for RDX and β-HMX, respectively, corresponding to the domains of phase stability of the room-temperature polymorphs for those materials. Comparison of the computed results to x-ray diffraction data reported by Olinger, Roof, and Cady[2] indicated good agreement for both the volumetric compression and the individual crystal lattice parameters, for all pressures considered. These quantities are sufficient to define a pressure-dependent bulk modulus and linear coefficients of isothermal compression.

More recently, we reported preliminary predictions of the anisotropic engineering moduli (Young's and shear) and Poisson ratios for crystalline RDX, for the same conditions of temperature and hydrostatic pressure considered in Ref. 1.[3] These predictions are based on formalism due to Parrinello and Rahman[4] in which the elastic stiffness tensor C_{ijkl} is expressed in terms of fluctuations in the elastic strain tensor $\langle \epsilon_{ij} \epsilon_{kl} \rangle$ for the material. The strain fluctuations were calculated using information generated during the course of the Monte Carlo realizations described in Ref. 1. The predicted moduli and Poisson ratios are in reasonable agreement with a very recent, experimental determination for RDX.[5]

In the present article, we report more extensive calculations of the crystal lattice parameters, anisotropic Young's and shear moduli, and Poisson ratios for RDX as functions of

[a)]Author to whom correspondence should be addressed; electronic mail: sewell@lanl.gov

both temperature and hydrostatic pressure. Specifically, we consider pressures in the domain 0 GPa$\leqslant p \leqslant$4 GPa and temperatures between $T=218$ K and $T=333$ K. Also, in the present calculations we employ recently published potential-energy surface parameters due to Sorescu, Rice, and Thompson,[6–9] which were specifically calibrated for RDX[6] and then shown to be transferrable to three HMX polymorphs,[7] as well as to a rather large set of additional nitramine-containing compounds.[8,9]

The outline for the remainder of the article is as follows: In Sec. II we briefly describe isothermal-isobaric Monte Carlo, the potential-energy surface used, and pertinent computational details. We then summarize the fluctuation formula from which the elastic coefficients, and hence the engineering parameters, are extracted. The results and accompanying discussion are provided in Sec. III. Finally, we summarize our conclusions and comment on directions for future work.

II. COMPUTATIONAL METHODS

A. Isothermal-isobaric Monte Carlo

The results were obtained using isothermal-isobaric (NpT) Monte Carlo methods. For a system of N rigid molecules, the ensemble average of macroscopic property $A(N,p,T)$ is therefore given by[10–12]

$$\langle A_{NpT}\rangle = \frac{\int d\mathbf{h}\int d\mathbf{s}\int d\mathbf{\Theta} A(\mathbf{s},\mathbf{\Theta};V(\mathbf{h}))e^{-\beta[U_N(\mathbf{s},\mathbf{\Theta})+pV(\mathbf{h})-(N/\beta)\ln V(\mathbf{h})]}}{\int d\mathbf{h}\int d\mathbf{s}\int d\mathbf{\Theta} e^{-\beta[U_N(\mathbf{s},\mathbf{\Theta})+pV(\mathbf{h})-(N/\beta)\ln V(\mathbf{h})]}}, \tag{1}$$

where $\mathbf{s}$ and $\mathbf{\Theta}$ are the molecular positions and orientations, respectively; U_N is the potential energy in terms of those variables; V is the volume; p is the scalar pressure; and $\beta = 1/\kappa T$. The positions and orientations in Eq. (1) are written in scaled coordinates, related to Cartesian coordinates $\mathbf{q}$ by the transformation $\mathbf{q}=\mathbf{hs}$, where $\mathbf{h}$ is the upper triangular matrix which transforms between the two coordinate systems. The columns of $\mathbf{h}$ are the lattice vectors $\mathbf{a}$, $\mathbf{b}$, and $\mathbf{c}$; the elements of $\mathbf{h}$ specify the size ($V=\det\mathbf{h}$) and shape of the volume under consideration.

The Monte Carlo estimate to Eq. (1) is the arithmetic average of the microscopic function of configuration $A(\mathbf{s},\mathbf{\Theta};V)$ which is taken over the states of a Markov chain in the configuration space of the system

$$A(N,p,T) = \lim_{M\to\infty} \frac{1}{M}\sum_{m=1}^{M} A(\mathbf{s}_m,\mathbf{\Theta}_m;V_m), \tag{2}$$

where the transition matrix between successive states is based on the potential energies $U_N(\mathbf{s}_m,\mathbf{\Theta}_m)$ in such a way as to assure detail balance and the equality of $A(N,p,T)$ with the actual ensemble average given above. The independent variables are the $6N$ molecular positions and orientations plus the six nonzero elements of $\mathbf{h}$.

In this work, the Markov chain was generated using a Metropolis algorithm[13] in which trial moves are accepted with probability $P=\min[\exp(-\Delta),1]$, where, for present state m and ''trial'' state $m+1$[10]

$$\Delta = \beta\{[U_N^{m+1}-U_N^m]+p[V^{m+1}-V^m]\} - N\ln(V^{m+1}/V^m). \tag{3}$$

B. Potential-energy surface

The intermolecular potentials used are of the form

$$U(\mathbf{R}) = \sum_A \sum_{B>A} \sum_{i\in A} \sum_{j\in B} [U_{\text{rep}}(\mathbf{R}_{ij}) + U_{\text{disp}}(\mathbf{R}_{ij}) + U_{\text{elec}}(\mathbf{R}_{ij})], \tag{4}$$

where A and B are molecules, and i and j denote particular atoms. The repulsion, dispersion, and electrostatic terms are written as

$$U_{\text{rep}} = A_{ij}e^{-B_{ij}R_{ij}}, \tag{5}$$

$$U_{\text{disp}} = -C_{ij}/R_{ij}^6, \tag{6}$$

$$U_{\text{elec}} = q_iq_j/R_{ij}, \tag{7}$$

where A, B, C, and q were taken from recent work due to Sorescu, Rice, and Thompson.[6] Those workers developed a set of potential parameters specifically for RDX by optimization of A and C for N-N and O-O interactions, using parameters due to Williams and co-workers[14,15] for all remaining X-X repulsion and dispersion interactions. Partial charges were obtained from an electronic structure calculation for the RDX asymmetric unit (one molecule) in the gas phase. Parameters for X-Y interactions were defined using traditional combination rules.

Although there are alternative functional forms and parametrizations for C, H, N, and O in the literature,[16–18] including one developed for flexible HMX,[18] the set of repulsion and dispersion parameters due to Sorescu, Rice, and Thompson is the only one specifically calibrated for RDX. Moreover, this set, taken together with molecule- and polymorph-specific partial charges, has been shown to be transferable to HMX polymorphs[7] as well as to a large set of additional nitramine-containing molecular crystals.[8,9] All potential parameters are provided in Ref. 6.

C. Strain fluctuations, elastic coefficients, and engineering moduli

In the theory of linear elasticity, the second-rank stress and strain tensors σ and ϵ are related through the elastic stiffness tensor $\mathbf{C}$ by[19]

$$\sigma_{ij}=C_{ijkl}\epsilon_{kl}, \tag{8}$$

where $i,j,k,l\in 1,2,3$. The inverse of the stiffness tensor is known as the compliance tensor, $\mathbf{S}=\mathbf{C}^{-1}$.

Parrinello and Rahman[4] have shown that the fluctuations in the elastic strain provide a direct measure of the isothermal compliance for a general anisotropic medium through the relation

$$S_{ijkl}=\langle \epsilon_{ij}\epsilon_{kl}\rangle \frac{\langle V\rangle}{\kappa T}, \tag{9}$$

where $\langle V\rangle$ is the mean volume and $\langle \epsilon_{ij}\epsilon_{kl}\rangle$ is the outer product of the strain tensor with itself. The strain tensor ϵ is given by

$$\epsilon=\tfrac{1}{2}(\mathbf{h_0'}^{-1}\mathbf{G}\mathbf{h_0}^{-1}-\mathbf{1}), \tag{10}$$

where $\mathbf{h_0}$ is the reference state of the sytsem and $\mathbf{G}=\mathbf{h}'\mathbf{h}$ is the metric tensor. A prime ($'$) indicates a matrix transpose.

The compliance in Eq. (9) is a fourth-rank tensor comprised of 81 elements. However, by taking advantage of the symmetry of ϵ, $\mathbf{S}$ can be rewritten in contracted (second-rank) form[20]

$$\mathbf{S}=\begin{pmatrix}\mathbf{M_1} & \mathbf{M_2}\\ \mathbf{M_3} & \mathbf{M_4}\end{pmatrix}, \tag{11}$$

where

$$\mathbf{M_1}=\begin{pmatrix}S_{1111} & S_{1122} & S_{1133}\\ S_{2211} & S_{2222} & S_{2233}\\ S_{3311} & S_{3322} & S_{3333}\end{pmatrix}, \tag{12}$$

$$\mathbf{M_2}=\begin{pmatrix}S_{1123}+S_{1132} & S_{1113}+S_{1131} & S_{1112}+S_{1121}\\ S_{2223}+S_{2232} & S_{2213}+S_{2231} & S_{2212}+S_{2221}\\ S_{3323}+S_{3332} & S_{3313}+S_{3331} & S_{3312}+S_{3321}\end{pmatrix}, \tag{13}$$

$$\mathbf{M_3}=2\begin{pmatrix}S_{2311} & S_{2322} & S_{2333}\\ S_{3111} & S_{3122} & S_{3133}\\ S_{1211} & S_{1222} & S_{1233}\end{pmatrix}, \tag{14}$$

$$\mathbf{M_4}=2\begin{pmatrix}S_{2323}+S_{2332} & S_{2313}+S_{2331} & S_{2312}+S_{2321}\\ S_{3123}+S_{3132} & S_{3113}+S_{3131} & S_{3112}+S_{3121}\\ S_{1223}+S_{1232} & S_{1213}+S_{1231} & S_{1212}+S_{1221}\end{pmatrix}. \tag{15}$$

For an orthotropic material,[21] $\mathbf{S}$ assumes the form

$$\mathbf{S}=\begin{pmatrix}\mathbf{A} & \mathbf{0}\\ \mathbf{0} & \mathbf{B}\end{pmatrix}, \tag{16}$$

where

$$\mathbf{A}=\begin{pmatrix}1/E_1 & -\nu_{21}/E_2 & -\nu_{31}/E_3\\ -\nu_{12}/E_1 & 1/E_2 & -\nu_{32}/E_3\\ -\nu_{13}/E_1 & -\nu_{23}/E_2 & 1/E_3\end{pmatrix} \tag{17}$$

and

$$\mathbf{B}=\begin{pmatrix}1/G_{23} & 0 & 0\\ 0 & 1/G_{31} & 0\\ 0 & 0 & 1/G_{12}\end{pmatrix} \tag{18}$$

contain the Young's moduli E_i and Poisson ratios ν_{ij}, and shear moduli G_{ij}, respectively.

Thus, the desired engineering coefficients can be obtained from an NpT Monte Carlo realization by calculation of the fluctuations of the strain tensor, expressed in terms of the instantaneous scaling matrix $\mathbf{h}$ and reference state $\mathbf{h_0}$ (defined as the element-wise arithmetic average of $\mathbf{h}$ determined from the realization).

D. Other computational details

At room temperature and atmospheric pressure, RDX crystallizes in the orthorhombic space group Pbca with $a=13.182$ Å, $b=11.574$ Å, $c=10.709$ Å, and $Z=8$ molecules per unit cell.[22] We included this number of molecules in our primary simulation cell, using the measured structure to define the molecular geometry and initial crystal structure. Periodic boundaries were used to simulate the infinite solid, and all interactions between molecules having center-of-mass separations of 20 Å or less were included in the energy evaluations.

One Monte Carlo cycle was defined to consist of five attempted rotations and translations per molecule plus 20 attempted variations in the size and shape of the primary simulation cell. Maximum displacements were adjusted to yield approximately a 50% acceptance probability for each kind of move. A complete realization consisted of 500 discarded warm-up cycles followed by a sequence of 10 000 production cycles. The final configuration from one realization was used as the initial configuration for the next. The thermodynamic states for two successive realizations were required to differ by (at least) either 60 K and 1.0 GPa or 30 K and 2.0 GPa.

Uncertainties reported below for lattice parameters correspond to the standard deviation of the mean, obtained from statistically independent subaverages computed along the Markov chain. The battery of analyses described by Hald[23] was used to determine a suitable length for the coarse-grained observations. Uncertainties for the moduli and Poisson ratios were obtained using a bootstrap method[24] in which the 10 000 Monte Carlo observations of $\mathbf{h}$ for a given (p,T) state were sampled randomly (with replacement) in batches of 2500 to obtain the compliance tensor, assuming that the sample pool of observations is representative of the population. Mean values and variances of the elements of the compliance tensor were obtained on the basis of 100 of these ''bootstrap cycles.'' Finally, standard error propagation techniques were used to obtain uncertainties for the elastic moduli and Poisson ratios derived from the compliance tensor [Eqs. (16)–(18)]. The error bars obtained in this way

TABLE I. Calculated stiffness matrix (GPa) and relative values C_{ij}/C_{11} for the case $T=276$ K, $p=2.0$ GPa. Relative values are in parentheses in the bottom half of the matrix structure.

49.570	14.310	17.690	0.187	−0.215	−0.313
	44.291	16.417	−0.462	0.209	−0.188
(1.000)		40.162	−0.227	−0.380	−0.054
(0.289)	(0.894)		13.186	0.304	−0.235
(0.357)	(0.331)	(0.810)		9.754	−0.198
(0.004)	(−0.009)	(−0.005)	(0.266)		12.018
(−0.004)	(0.004)	(−0.008)	(0.006)	(0.197)	
(−0.006)	(−0.004)	(−0.001)	(−0.005)	(−0.004)	(0.242)

were found to be relatively insensitive to the precise values chosen for the bootstrap parameters. In all cases, error bars correspond to one standard deviation.

III. RESULTS AND DISCUSSION

We have performed rigid-molecule isothermal-isobaric Monte Carlo realizations for crystalline RDX in order to extract the isothermal compliance tensor and hence the anisotropic engineering coefficients. A set of temperatures and hydrostatic pressures relevant to the development of improved mesomechanical descriptions of energetic materials under weak to moderate stress loading was considered. An additional benefit of the calculations is new pressure-volume-temperature (pVT) equation of state information. While the calculations described here were performed in the rigid-molecule approximation, previous agreement[1] with experiment using a similar potential-energy parametrization suggests that this is not too severe an approximation for the quantities discussed below.

A. Elastic constants and derived parameters

The calculated stiffness matrix for ($p=2.0$ GPa, $T=276$ K) is given in Table I. Also included in Table I is the ratio C_{ij}/C_{11}. (C_{11} is the largest element of $\mathbf{C}$ for the case considered.) Since the matrix is symmetric, only the upper half is shown. It is seen that the form expected for orthotropic materials [Eqs. (16)–(18)] is well satisfied.[25] Each of the elements that should be zero for an orthotropic material is at most 5% of the smallest formally nonzero one, and most of them are much smaller. Similar results were obtained for other pressures and temperatures.

The calculated elastic moduli are collected in Table II. Plots of the pressure dependence ($T=276$ K) and of the temperature dependence ($p=0.0$ GPa) are shown in Figs. 1 and 2. The magnitudes of the Young's and shear moduli (E_i and G_{ij}) at zero pressure are reasonable for organic molecular solids, and are seen to increase dramatically with increasing hydrostatic pressure (Fig. 1). This is expected due to the significant (~15%) bulk compression that occurs at the

TABLE II. Calculated Young's and shear moduli as $f(p,T)$. Units are GPa. Uncertainties in the last digit are in parentheses.

T (K)	p (GPa)	E_1	E_2	E_3	G_{23}	G_{31}	G_{12}
218	0.0	27.3(8)	27.0(8)	17.4(4)	9.6(3)	6.0(2)	9.1(3)
	1.0	30.3(8)	33.1(9)	28.2(8)	13.0(3)	8.5(2)	11.8(4)
	2.0	39(1)	35(1)	31.0(8)	12.0(3)	9.5(3)	12.3(4)
	3.0	65(2)	63(2)	41(1)	20.7(5)	11.2(3)	21.3(6)
	4.0	72(2)	85(3)	71(2)	25.4(7)	19.0(5)	26.2(8)
247	0.0	26.0(7)	25.5(7)	16.6(4)	9.1(3)	5.5(2)	8.9(3)
	1.0	32.5(8)	33(1)	29.3(8)	12.9(4)	8.1(2)	12.0(4)
	2.0	38(1)	36(1)	28.8(8)	13.5(4)	9.3(3)	12.4(4)
	3.0	63(2)	59(2)	41(1)	19.7(6)	11.3(3)	20.6(6)
	4.0	70(2)	83(3)	62(2)	26.3(6)	17.1(5)	26.7(7)
276	0.0	24.8(8)	23.0(8)	16.9(5)	8.6(2)	5.7(2)	8.3(3)
	1.0	31.6(9)	32.3(8)	29.9(8)	13.0(4)	8.2(2)	11.3(3)
	2.0	40(1)	36(1)	30.6(9)	13.1(3)	9.7(3)	12.0(3)
	3.0	58(2)	56(1)	41(1)	18.8(5)	11.5(3)	18.3(5)
	4.0	77(2)	78(2)	64(2)	24.1(7)	16.8(5)	25.0(9)
304	0.0	24.2(7)	21.1(6)	15.4(4)	8.4(2)	5.3(2)	7.6(2)
	1.0	29.8(8)	32.1(9)	26.6(7)	12.7(4)	8.0(2)	11.6(4)
	2.0	36(1)	35(1)	29.7(8)	12.9(3)	9.5(3)	12.6(3)
	3.0	58(2)	56(2)	38(1)	19.0(6)	11.4(3)	19.3(7)
	4.0	70(2)	74(2)	57(2)	25.7(7)	17.2(5)	24.9(7)
333	0.0	22.2(7)	20.2(6)	14.3(4)	7.4(2)	5.1(1)	7.9(2)
	1.0	31.1(9)	32.1(9)	26.0(7)	11.7(3)	7.7(2)	10.7(3)
	2.0	41(1)	37(1)	31(1)	13.4(4)	9.9(3)	12.3(4)
	3.0	57(2)	54(2)	40(1)	18.4(5)	11.5(3)	18.5(5)
	4.0	70(2)	74(2)	56(2)	24.1(7)	16.5(4)	25.1(7)

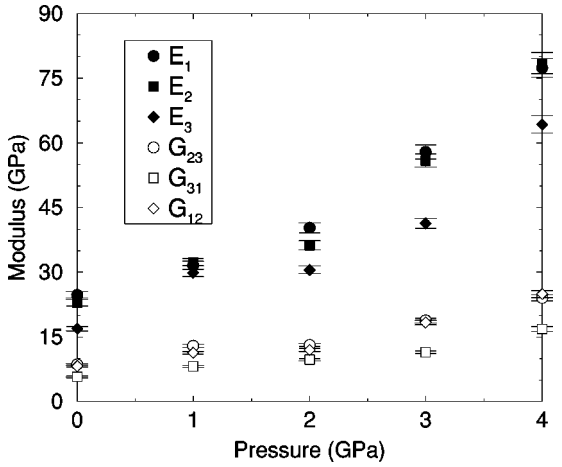

FIG. 1. The calculated Young's and shear moduli for RDX are shown as a function of hydrostatic pressure for a fixed temperature of $T=276$ K. Individual moduli are identified in the figure legend.

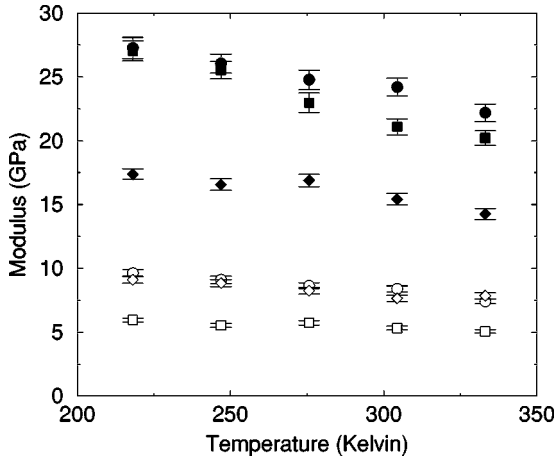

FIG. 2. The calculated Young's and shear moduli for RDX are shown as a function of temperature for a fixed hydrostatic pressure of $p=0.0$ GPa. Individual moduli are identified using the same scheme as in Fig. 1.

highest pressures.[1,2] Anisotropy among the moduli is evident, although not prominently so. In particular, E_3 and G_{31} are approximately 2/3–3/4 the values of the remaining Young's and shear moduli. The relative increases in the shear moduli with pressure are smaller than for the Young's moduli. The temperature dependence of the moduli is relatively weak (Fig. 2), and is near the limit of precision of our calculations. However, in most cases, the moduli decrease with increasing temperature (Table II).

The six Poisson ratios (ν) are tabulated in Table III. Plots of the pressure and temperature dependence of two of them (ν_{21} and ν_{13}) are provided in Fig. 3. For clarity of presentation, the results for each successive temperature are offset by 0.025 GPa from the preceding one. The qualitative features of ν_{21} and ν_{13} are representative of the remaining four. The relative uncertainties for ν_{ij} are significantly larger than for either E_i or G_{ij}, and the temperature dependence is not resolved in the present calculations. Different ν_{ij} apparently have distinct pressure dependencies, including statistically significant non-monotonicities. There is a weak positive pressure dependence in the ''isotropic'' Poisson ratio, defined as the arithmetic average over all six ν_{ij} and all five temperatures, as shown by the bold dot-dash line in Fig. 3.

For an isotropic material, the bulk modulus K is given by

TABLE III. Calculated Poisson ratios as $f(p,T)$. Uncertainties in the last digit are in parentheses.

T (K)	p (GPa)	ν_{21}	ν_{31}	ν_{12}	ν_{32}	ν_{13}	ν_{23}
218	0.0	0.20(2)	0.17(2)	0.20(3)	0.19(2)	0.27(3)	0.30(3)
	1.0	0.24(3)	0.32(3)	0.22(3)	0.21(2)	0.34(3)	0.25(3)
	2.0	0.18(3)	0.27(2)	0.20(3)	0.29(3)	0.34(3)	0.33(3)
	3.0	0.22(3)	0.20(2)	0.22(3)	0.27(2)	0.31(3)	0.42(4)
	4.0	0.31(3)	0.25(3)	0.26(3)	0.25(3)	0.25(3)	0.31(3)
247	0.0	0.17(2)	0.20(2)	0.18(2)	0.19(2)	0.31(4)	0.29(3)
	1.0	0.23(3)	0.25(3)	0.23(3)	0.25(3)	0.28(3)	0.28(3)
	2.0	0.19(2)	0.29(3)	0.20(2)	0.28(2)	0.38(3)	0.35(3)
	3.0	0.21(2)	0.20(2)	0.22(3)	0.27(2)	0.31(3)	0.39(4)
	4.0	0.29(3)	0.26(3)	0.25(3)	0.22(3)	0.30(3)	0.29(3)
276	0.0	0.19(3)	0.15(2)	0.20(3)	0.22(2)	0.22(3)	0.30(3)
	1.0	0.25(3)	0.27(3)	0.24(3)	0.25(3)	0.28(3)	0.27(3)
	2.0	0.17(2)	0.28(3)	0.19(3)	0.28(3)	0.36(4)	0.33(3)
	3.0	0.21(3)	0.24(2)	0.22(3)	0.27(2)	0.33(3)	0.36(3)
	4.0	0.24(3)	0.22(3)	0.24(3)	0.28(3)	0.26(3)	0.34(4)
304	0.0	0.17(2)	0.16(2)	0.20(3)	0.22(3)	0.25(4)	0.30(4)
	1.0	0.25(3)	0.29(3)	0.23(3)	0.22(3)	0.33(3)	0.27(3)
	2.0	0.20(3)	0.32(3)	0.20(3)	0.28(3)	0.38(4)	0.33(4)
	3.0	0.17(2)	0.25(2)	0.18(2)	0.29(2)	0.38(4)	0.43(4)
	4.0	0.28(3)	0.24(3)	0.27(3)	0.28(3)	0.29(3)	0.36(3)
333	0.0	0.16(2)	0.18(2)	0.18(3)	0.20(2)	0.28(3)	0.28(3)
	1.0	0.23(3)	0.23(3)	0.23(3)	0.25(3)	0.28(3)	0.31(3)
	2.0	0.18(2)	0.26(3)	0.20(3)	0.28(3)	0.34(3)	0.34(3)
	3.0	0.20(2)	0.25(2)	0.21(3)	0.28(3)	0.35(3)	0.38(4)
	4.0	0.26(3)	0.27(2)	0.24(3)	0.25(2)	0.33(3)	0.33(3)

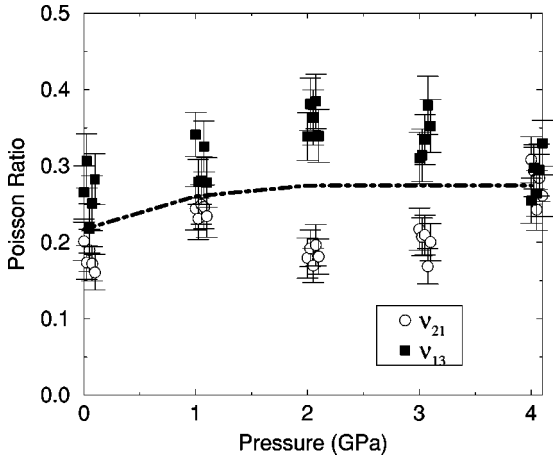

FIG. 3. The calculated Poisson ratios ν_{21} and ν_{13} for RDX are shown as a function of hydrostatic pressure (abscissa) and temperature (parametric variable). Values for successively higher temperatures at a given pressure are offset from one another by 0.025 GPa for clarity of presentation. The heavy dot-dash line is the average of all six Poisson ratios, and over all five temperatures, at a given pressure.

$$K=\frac{E}{3(1-2\nu)}.$$

If, for the case $T=304\,\mathrm{K}$ and $p=0.0\,\mathrm{GPa}$, we compute the arithmetic average of the Young's moduli and Poisson ratios to obtain isotropic values $E=20.2\,\mathrm{GPa}$ and $\nu=0.22$, then we predict a zero-pressure bulk modulus of $K=12\,\mathrm{GPa}$, in good agreement with the experimental value $K_{\mathrm{expt}}=13.0\,\mathrm{GPa}$ due to Olinger, Roof, and Cady.[2] The entire set of elastic constants for RDX has been measured very recently, and will appear in a forthcoming publication.[5] The comparison between experiment and calculation ($T=304\,\mathrm{K}$, $p=0.0\,\mathrm{GPa}$) is favorable but not outstanding. The resulting anisotropic Young's and shear moduli are 130% and 116% of the respective experimental values (Voigt averages); the average Poisson ratio is 80% of the experimental number. Although the elastic moduli we predict are somewhat larger than the experimental values, this is evidently balanced by a smaller Poisson ratio, to yield a bulk modulus within 4% of experiment.

B. The *pVT* equation of state and derived parameters

The pV equation of state for RDX has been measured ($T=295\,\mathrm{K}$, $0\,\mathrm{GPa}\leqslant p\leqslant 9.19\,\mathrm{GPa}$) by Olinger and co-workers.[2] A phase transition was identified above 4 GPa, but the structure of the high-pressure polymorph has yet to be determined (although it has been studied spectroscopically[26]). Here we present calculated unit cell volumes and lattice lengths for 25 uniformly spaced p-T pairs ($0.0\,\mathrm{GPa}\leqslant p\leqslant 4.0\,\mathrm{GPa}$ and $218\,\mathrm{K}\leqslant T\leqslant 333\,\mathrm{K}$). We do not report lattice angles since the averages never deviate significantly from 90°. The results, which are collected in Table IV, are sufficient to allow for predictions of linear and volumetric coefficients of isothermal compressibility and thermal expansion on the $p-T$ surface. Values for some of these are contained in Tables V and VI, where we also include the available experimental data. For purposes of comparison in the remainder of this section, the calculated results were standardized to a temperature of $T=295\,\mathrm{K}$. Values corresponding to $T=295\,\mathrm{K}$ were obtained using least square fits of the lattice parameters as $f(T;p)$. In cases where hydrostatic compression results are compared to experiment, we ignore the 0.05 GPa difference between the two.

TABLE IV. Calculated lattice lengths and unit cell volume as $f(p,T)$. Uncertainties in the last digit are given in parentheses.

T (K)	p (GPa)	a (Å)	b (Å)	c (Å)	Volume (Å^3)
218	0.0	13.376(3)	11.715(2)	10.706(3)	1676.9(3)
	1.0	13.160(4)	11.529(1)	10.458(3)	1586.1(3)
	2.0	12.974(4)	11.365(2)	10.310(3)	1519.7(3)
	3.0	12.859(3)	11.255(1)	10.172(2)	1472.0(2)
	4.0	12.775(3)	11.203(1)	10.065(2)	1440.3(1)
247	0.0	13.389(3)	11.730(2)	10.720(4)	1682.9(3)
	1.0	13.166(3)	11.537(2)	10.462(3)	1588.6(3)
	2.0	12.979(5)	11.374(2)	10.314(3)	1522.1(3)
	3.0	12.866(3)	11.261(2)	10.175(2)	1473.9(2)
	4.0	12.774(3)	11.203(1)	10.076(2)	1441.7(1)
276	0.0	13.400(3)	11.741(2)	10.739(4)	1688.6(4)
	1.0	13.169(4)	11.545(2)	10.472(3)	1591.5(3)
	2.0	13.004(4)	11.382(2)	10.311(3)	1525.6(3)
	3.0	12.875(4)	11.268(2)	10.180(3)	1476.4(2)
	4.0	12.785(2)	11.203(1)	10.076(2)	1443.0(2)
304	0.0	13.410(3)	11.758(2)	10.756(4)	1694.8(4)
	1.0	13.176(5)	11.552(2)	10.483(4)	1594.8(3)
	2.0	12.994(5)	11.390(2)	10.324(4)	1527.5(3)
	3.0	12.873(4)	11.273(2)	10.190(3)	1478.2(2)
	4.0	12.790(3)	11.205(2)	10.083(3)	1444.6(2)
333	0.0	13.424(3)	11.775(2)	10.771(5)	1701.4(5)
	1.0	13.178(4)	11.562(2)	10.495(4)	1598.2(3)
	2.0	13.020(4)	11.395(2)	10.323(3)	1530.9(3)
	3.0	12.881(4)	11.280(2)	10.190(3)	1480.1(2)
	4.0	12.786(3)	11.210(1)	10.093(2)	1446.2(2)

TABLE V. Illustrative parameters pertaining to isothermal compression.

	a (Å)		b (Å)		c (Å)		V (Å^3)	
p (GPa)	Calc.[a,b]	Expt.[a,c]	Calc.[a,b]	Expt.[a,c]	Calc.[a,b]	Expt.[a,c]	Calc.[a,b]	Expt.[a,c]
0.0	13.407	13.20	11.754	11.60	10.750	10.72	1693.0	1641.4
	a/a_0		b/b_0		c/c_0		V/V_0	
T (K)[d]	Calc.	Expt.[c]	Calc.	Expt.[c]	Calc.	Expt.[c]	Calc.	Expt.[c]
218	0.955	⋯	0.956	⋯	0.940	⋯	0.859	⋯
295[b]	0.954	0.960	0.954	0.942	0.938	0.936	0.853	0.846
333	0.952	⋯	0.952	⋯	0.937	⋯	0.850	⋯

[a]$T=295$ K.
[b]Obtained from linear least squares fit.
[c]Reference 2.
[d]For a pressure of 4 GPa.

The isothermal compression is in good agreement with the experimental data (Table V). Specifically, the percent errors in the calculated lattice lengths and unit cell volume at $p=0.0$ GPa are 1.6%, 1.3%, and 0.3% for a, b, and c, respectively, and 3.1% for the unit cell volume. A comparison of the linear and volumetric compression x/x_0 [where $x=a,b,c$, or V, $x=x(p)$, and $x_0=x(p=0)$] along the $T=295$ K isotherm yields errors of -0.6%, 1.3%, and 0.2% for the lattice lengths, and 0.8% for the unit cell volume. Temperature effects on the hydrostatic compression are small for the temperature domain considered: the average percent difference in x/x_0 for the two limiting temperatures is only 0.3% and 1.1% for lattice lengths and unit cell volume, respectively.

The coefficient of thermal expansion (CTE) is given by $\alpha=x^{-1}[\partial x(T)/\partial T]|_p$. We fit our results to this using linear regression to obtain $x(T;p)$ and hence a temperature-dependent CTE for each lattice parameter (Table VI). The precision of the results does not warrant the use of a higher-order fitting form. Cady[27] has measured the linear and volumetric CTE of RDX at atmospheric pressure and expressed these quantities as a fifth-degree polynomial in temperature. The comparison to experiment is not as good as for isothermal compression (Table VI). Taking into account Cady's choice of a, b, and c axes, and retaining only terms through third degree, the percent errors are 15.7%, -49.1%, and -31.8% for the linear CTEs along a, b, and c. The percent error in the volumetric CTE is -34.6%. These values are comparable to those given previously by Sorescu, Rice, and Thompson[6] in the initial presentation of their potential set for RDX. We find a strong dependence of the CTE on pressure, as is shown at the bottom of Table VI. For example, we predict the volumetric CTE at $T=295$ K to decrease by a factor of 3.5 in passing from $p=0.0$ GPa to $p=4.0$ GPa. Although one obviously cannot make an accurate prediction of the absolute magnitude of the CTEs based on our results, the good agreement we obtain for isothermal compression suggests that it might be possible to map the calculated pressure dependence of the volumetric CTE onto an effective temperature curve using a calibration that accounts for the error in the predicted CTE.

Using neutron scattering techniques, Dick and von Dreele[28] have observed pressure-induced distortions of up to 8° in torsional angles for the high explosive pentaerythritol tetranitrate (PETN) hydrostatically loaded to 4.28 GPa in a diamond anvil cell. Since both RDX and HMX have low frequency (less than 200 cm^{-1}), anharmonic molecular modes[29,30] that couple with phonon modes in the material,[31] the applicability of rigid molecules for the temperatures, pressures, and properties of interest in the present work needs to be more carefully assessed. We hope to address this issue in future publications.

IV. CONCLUSIONS

Isothermal-isobaric Monte Carlo calculations were used within an all-atom rigid-molecule framework to compute the elastic coefficient tensor C_{ijkl} and derived anistropic engineering moduli and Poisson ratios for crystalline RDX as a function of temperature and hydrostatic pressure. The elastic coefficients were computed on the basis of formalism due to Parrinello and Rahman[4] in which the C_{ijkl} are obtained in terms of fluctuations of the strain tensor. An additional product of the calculations is new pVT equation of state information from which quantities such as linear and volumetric coefficients of isothermal compression and thermal expansion can be obtained.

Assuming an orthotropic form for the compliance matrix (a legitimate assumption), we computed the Young's and shear moduli, and the Poisson ratios as a function of hydrostatic pressure and temperature in the domain $0\ \text{GPa}\leqslant p$

TABLE VI. Coefficients of thermal expansion. The temperature is $T=295$ K.

	α_a (°C^{-1})		α_b (°C^{-1})		α_c (°C^{-1})		α_V (°C^{-1})	
p (GPa)	Calc.	Expt.[a]	Calc.	Expt.[a]	Calc.	Expt.[a]	Calc.	Expt.[a]
0.0	3.02×10^{-5}	2.61×10^{-5}	4.42×10^{-5}	8.68×10^{-5}	5.36×10^{-5}	7.86×10^{-5}	1.25×10^{-4}	1.91×10^{-4}
4.0	1.01×10^{-5}	⋯	4.79×10^{-6}	⋯	2.15×10^{-5}	⋯	3.55×10^{-5}	⋯

[a]Reference 27.

$\leqslant 4$ GPa and $218\,\mathrm{K} \leqslant T \leqslant 333\,\mathrm{K}$. The results for room temperature and pressure are in reasonable, though not outstanding, agreement with a very recent, unpublished experimental determination of these quantities for RDX.[5] The moduli are predicted to increase significantly at higher pressures, which is physically sensible given the $\sim 15\%$ compression that occurs at the upper end of the pressure domain considered. The results indicate thermal ''softening'' of the crystal as the temperature is increased, although the extent of this softening is not monotonic with pressure, nor is it well resolved in all circumstances.

The calculated linear and volumetric isothermal compression $T = 275\,\mathrm{K}$ is in good agreement with experimental results, with errors of 3% or less. The temperature dependence of these quantities is predicted to be small over the domain studied. By contrast, the coefficients of thermal expansion (CTEs) are not in close agreement with experiment. Errors in the linear CTEs range from -49.1% to $+15.7\%$, while that for the volumetric CTE is -34.6%. This discrepancy has also been noted by the developers of the potential set used, and may arise in part due to the use of rigid molecules. We find a rather large pressure dependence of the CTEs, $\sim$ a factor of 3–5 in passing from $p = 0$ GPa to $p = 4$ GPa at constant temperature.

Calculations similar to those described here are under way for HMX. Future investigations are planned to explore the limits of temperature and pressure for which the assumption of rigid molecules is valid.

ACKNOWLEDGMENTS

This research was supported by the U.S. Department of Energy, under the auspices of the Los Alamos high-explosives component of the Accelerated Strategic Computing Initiatve (ASCI). C.M.B. was a graduate research assistant at Los Alamos during the summer of 1998. T.D.S. thanks Sam Shaw and Jerry Erpenbeck for useful discussions over the course of this work.

[1] T. D. Sewell, J. Appl. Phys. **83**, 4142 (1998).
[2] B. Olinger, B. Roof, and H. Cady, Symposium International Sur le Comportement Des Milieux Denses Sous Hautes Pressions Dynamiques, Paris, France, 1978, p. 3.
[3] C. M. Bennett and T. D. Sewell, to appear in Proceedings of the Eleventh Symposium (International) on Detonation, Snowmass, Co, 1998.
[4] M. Parrinello and A. Rahman, J. Chem. Phys. **76**, 2662 (1982).
[5] S. Saussühl (private communication); to be published in Z. Kristallogr.
[6] D. C. Sorescu, B. M. Rice, and D. L. Thompson, J. Phys. Chem. B **101**, 798 (1997).
[7] D. C. Sorescu, B. M. Rice, and D. L. Thompson, J. Phys. Chem. B **102**, 6692 (1998).
[8] D. C. Sorescu, B. M. Rice, and D. L. Thompson, J. Phys. Chem. B **102**, 948 (1998).
[9] D. C. Sorescu, B. M. Rice, and D. L. Thompson, J. Phys. Chem. A **102**, 8386 (1998).
[10] W. W. Wood, in *Physics of Simple Fluids*, edited by H. N. V. Temperley, J. S. Rowlinson, and G. S. Rushbrooke (North-Holland, Amsterdam, 1968), Chap. 5, p. 115.
[11] M. Parrinello and A. Rahman, J. Appl. Phys. **52**, 7182 (1981).
[12] S. Yashonath and C. N. R. Rao, Mol. Phys. **54**, 245 (1985).
[13] N. Metropolis, A. W. Rosenbluth, M. N. Rosenbluth, A. H. Teller, and E. Teller, J. Chem. Phys. **21**, 1087 (1953).
[14] D. E. Williams and S. R. Cox, Acta Crystallogr., Sect. B: Struct. Sci. **40**, 404 (1984).
[15] S. R. Cox, L. Y. Hsu, and D. E. Williams, Acta Crystallogr., Sect. A: Cryst. Phys., Diffr., Theor. Gen. Crystallogr. **37**, 293 (1981).
[16] A. J. Pertsin and A. I. Kitaigorodsky, *The Atom-Atom Potential Method. Applications to Organic Molecular Solids* (Springer, Berlin, 1987).
[17] S. L. Price, in *Reviews in Computational Chemistry*, edited by K. B. Lipkowitz and D. B. Boyd (Wiley-VCH, New York, 1999), Vol. 14, p. 225.
[18] G. D. Smith and R. K. Bharadwaj, J. Phys. Chem. B **103**, 3570 (1999).
[19] H. H. E. Leipholz, *Theory of Elasticity* (Noordhoff, Leyden, 1974).
[20] S. W. Tsai, AFML Technical Report No. AFML-TR-66-149, November, 1966.
[21] That is, one in which the material properties are different in three mutually perpendicular directions.
[22] C. S. Choi and E. Prince, Acta Crystallogr., Sect. B: Struct. Crystallogr. Cryst. Chem. **28**, 2857 (1972).
[23] A. Hald, in *Statistical Theory with Engineering Applications* (Wiley, New York, 1952), Chap. 13, p. 338.
[24] P. Diaconis and B. Efron, Sci. Am. **248**, 166 (1983).
[25] The forms of the stiffness and compliance tensors share the same symmetry and have zero elements in the same locations.
[26] B. J. Baer, J. Oxley, and M. Nicol, High Press. Res. **2**, 99 (1990).
[27] H. H. Cady, J. Chem. Eng. Data **17**, 369 (1972).
[28] J. J. Dick and R. B. von Dreele, in *Shock Compression of Condensed Matter—1997*, edited by S. C. Schmidt, D. P. Dandekar, and J. W. Forbes (AIP, Woodbury, NY, 1998), p. 827.
[29] N. F. Fell, Jr, J. A. Vanderhoff, R. A. Pesce-Rodriguez, and K. L. McNesby, J. Raman Spectrosc. **29**, 165 (1998).
[30] H. V. Brand (unpublished).
[31] J. Eckert (private communication).